Guo *et al. Cell Communication and Signaling* (2025) 23:148
https://doi.org/10.1186/s12964-025-02148-5

Cell Communication and Signaling

RESEARCH Open Access

Platelet glycoprotein VI promotes folic acid-induced acute kidney injury through interaction with tubular epithelial cell-derived galectin-3

Ya-Wei Guo[1,2], Qi Luo[1,2], Meng Lu[1,2], Xiang-Bin Zeng[1,2], Yu-Min Zhang[1,2], Yue-Ling Lin[1,2], Xu-Ran Guo[1,2], Rong Ma[1,2] and Zhang-Yin Ming[1,2,3*]

Abstract

Background Acute kidney injury (AKI) is defined by a significant reduction in renal function, which subsequently impairs coagulation and activates the inflammatory immune response, ultimately resulting in damage to renal tubular epithelial cells (TECs). Platelets are crucial in mediating both inflammatory and coagulation processes. While it is established that platelet activation contributes to the progression of AKI, the precise mechanisms underlying this relationship remain largely unclear.

Methods We investigated platelet function in folic acid-induced acute kidney injury (FA-AKI) and examined the effects of galectin-3, a protein derived from renal tubular epithelial cells (TECs), on its interaction with platelet glycoprotein VI (GPVI). This interaction was assessed through the analysis of monocyte migration, macrophage polarization, and the generation of monocyte-platelet aggregation. Additionally, we utilized platelet GPVI-specific knockout mice in conjunction with TD139, a small-molecule inhibitor of galectin-3, to explore the effects of inhibiting the galectin-3-GPVI interaction on FA-AKI.

Results In the current study, we observed that mouse platelets displayed hyperactivity in the context of functional acute kidney injury (FA-AKI). This hyperactivity was linked to the interaction between galectin-3, which is derived from damaged renal tubular epithelial cells (TECs), and the glycoprotein VI (GPVI) on platelets. Our findings indicated a heightened interaction between activated platelets and monocytes, along with an increase in monocyte-platelet aggregation (MPA) within the circulation. The increased infiltration of monocytes and platelets in renal tissue was further validated through CD41 and CD68 immunofluorescence techniques. Additionally, the interaction between galectin-3 and platelet GPVI was shown to facilitate monocyte migration, promote M1-type macrophage polarization, and enhance phagocytic activity. The galectin-3 inhibitor TD139 significantly suppressed monocyte-platelet aggregation (MPA), reduced inflammatory responses, and extended the survival of mice with acute kidney injury (AKI).

*Correspondence:
Zhang-Yin Ming
zyming@hust.edu.cn

Full list of author information is available at the end of the article

Conclusions These findings suggest that galectin-3, which is released from damaged cells during acute kidney injury (AKI), exacerbates renal inflammation and tissue damage by activating platelets through glycoprotein VI (GPVI). This activation enhances interactions between monocytes and platelets, ultimately leading to the formation of monocyte-platelet aggregates (MPA) and the polarization of M1 macrophages.

Keywords Platelets, GPVI, Galectin-3, Acute kidney injury, Monocyte-platelet aggregates, Macrophage

Background

Acute kidney injury (AKI) is a prevalent clinical condition. Despite significant advancements in understanding its underlying pathogenesis, recent epidemiological studies indicate a continuing rise in the incidence of AKI [1, 2]. The primary pathological features include injury and death of renal tubular epithelial cells (TECs), with inflammatory responses between injured tubular cells and immune cells, such as platelets, contributing to the further exacerbation of renal damage [3, 4]. However, the precise mechanism by which injury to renal TECs initiates renal inflammation through platelets remains unclear.

Platelet glycoprotein VI (GPVI) is a critical adhesion receptor located on the surface of platelets, playing a vital role in platelet activation [5]. GPVI binds to collagen and activates platelets via immunoreceptor tyrosine activation motif (ITAM) signaling. This mechanism is significant in both physiological and pathological processes, including thrombosis, hemostasis, inflammation, and other related conditions [6, 7]. Saori et al. [8] found that in rhabdomyolysis-induced AKI, heme released from necrotic myocytes interacted with GPVI to induce platelet activation, thereby facilitating the formation of extracellular traps in renal macrophages. In addition to its essential role in inflammation, GPVI is also involved in tumor metastasis [9]. A recent study revealed that galectin-3, produced by tumor cells, binds to platelet GPVI, thereby promoting distant tumor metastasis [10]. Concurrently, numerous studies have demonstrated that galectin-3 is highly expressed in AKI and shows a positive correlation with the severity of kidney damage [11, 12]. However, it remains unclear whether galectin-3, originating from renal TECs injury, can interact with GPVI to exacerbate renal burden.

Platelets occupy a unique position in peripheral blood and can mediate tissue inflammation by interacting with various immune cell populations through distinct receptors [13]. Increased levels of circulating platelet-leukocyte aggregates have been observed in conditions such as myocardial infarction [14], atherosclerosis [15] and angina pectoris [16]. Targeting and blocking platelet-immune cell interactions has proven to be an effective strategy for disease mitigation. However, the role of platelet-immune cell complexes in AKI remains poorly understood. In the present study, it was found that MPA was significantly increased in FA-AKI. Platelet activation through the interaction of GPVI with galectin-3 derived from renal TECs plays a critical role in this process. Furthermore, the inhibition of galectin-3 by TD139 has been identified as a promising new therapeutic agent for the treatment of FA-AKI.

Methods

Mouse models

GPVI ($Gp6^{-/-}$) knockout mice with a C57BL/6 background were acquired from Cyagen (Suzhou) Biotechnology Co. $Gp6^{+/+}$ littermate mice were bred in our delivery facility and used as controls. Experiments using male (6–8 weeks) animals were approved by the Animal Experimentation Ethics Committee of Tongji Medical College, Huazhong University of Science and Technology. The experiments were conducted in accordance with the eighth edition of the Guide for the Care and Use of Laboratory Animals. Animals were housed in an environment with controlled light and temperature, and they had unrestricted access to food and water. In the FA-AKI group, mice received an intraperitoneal injection of 250 mg/kg of folic acid, while the control group received an equal volume of 0.3 mol/L $NaHCO_3$ via intraperitoneal injection [17]. Following a 24 h treatment period, blood and kidney tissue samples were collected from the mice.

Renal function assessment

Blood samples were collected 24 h following an intraperitoneal injection of 250 mg/kg folic acid or an equivalent volume of 0.3 mol/L $NaHCO_3$ to evaluate the renal function of mice. Serum creatinine (CRE) and blood urea nitrogen (BUN) levels in the blood samples were measured using creatinine (Nanjing Jiancheng, C011-2-1, Nanjing, China) and blood urea nitrogen assay kits (Nanjing Jiancheng, C013-1-1, Nanjing, China), respectively, following the manufacturer's instructions. Calculated by comparing kidney weight to mouse body weight. The kidney/body weight ratio reflects changes in kidney size and weight and is an important indicator for assessing the pathological state of the kidneys.

Periodic Acid-Schiff (PAS), haematoxylin&eosin (HE) staining and Sirius red staining

To assess the extent of tissue damage, kidney tissues were immediately fixed in 4% paraformaldehyde overnight. PAS, HE (24 h) and Sirius red (4 weeks) staining

were performed on paraffin sections at 5 μm by following the manufacturer's protocol with the PAS (Servicebio, G1008, Wuhan, China), Sirius red kit (Servicebio, G1018, Wuhan, China) and HE (Servicebio, G1005, Wuhan, China) kits. The assessment of tissue damage was conducted with blinding and was rated based on the proportion of affected tubules: 0 representing no damage; 1 indicating less than 25% damage; 2 corresponding to 25–50% damage; 3 for 50–75% damage; and 4 for damage exceeding 75%, as previously reported [18].

Preparation of platelet

Mice platelets were prepared as previously described [19, 20]. Briefly, venous blood from mice was into sodium citrate (3.8%) in a ratio of 9: 1 (v/v), diluted with an equal volume Tyrode's buffer (137 mM NaCl, 2.5 mM KCl,13.8 mM $NaHCO_3$, 0.36 mM NaH_2PO_4, 5.5 mM glucose and 20 mM HEPES, pH 7.4), and centrifuged at 160 g for 15 min. Platelets were collected by centrifuged the Platelet-rich plasma (PRP) at 550 g for 10 min in the presence of 1 μM PGE1 (Sigma, P5515, USA), and then platelets were resuspended with 1 × Tyrode's buffer for subsequent experiments.

Platelet functional studies

The concentration of platelets resuspended in Tyrode's buffer was adjusted to 300×10^9/L. Platelet aggregation response to agonists (collagen and thrombin) was measured using a luminescent aggregometer (Model 700 Chrono-Log) at 37 °C and 1000 rpm. ATP release was measured using Chrono-lume reagent, and secretion of platelet-dense granules was monitored.

For clot retraction, washed platelets were normalized to a concentration of 300×10^9/L, and then 20 mg/mL of fibrinogen was added to 0.5 mL of platelets. Clot retraction was induced by thrombin (2U/mL) at 37 °C and monitored by taking pictures with a digital camera at the indicated times. The percentage of retraction was counted using ImageJ software (Media Cybernetics Inc).

For platelet spreading, 250 μL of platelets at a concentration of 5×10^9/L were incubated at 37 °C onto glass coverslips coated with 50 μg/mL fibrinogen. After platelets were fixed, permeabilized and blocked with 1% BSA, they were stained with rhodamine-labelled phosphatidylinositide-like proteins as described previously [20]. Platelets spreading on fibrinogen-coated glass coverslips were photographed with an Olympus optical fluorescence microscope, and the platelet spreading area of random images was calculated using ImageJ software (Media Cybernetics Inc).

Immunohistochemical (IHC) staining

Kidney sections were baked at 60 °C for fixation, deparaffinized with an environmentally friendly tissue deparaffinizing solution (Servicebio, G1128, Wuhan, China) and citrate buffer for antigen repair. These kidney sections were incubated overnight at 4 °C with anti-galectin-3 (Abcam, ab76245, UK) 1:100 primary antibody. The secondary antibody was incubated at room temperature for 1 h. After DAB re-staining, the sections were re-incubated with hematoxylin and imaged randomly.

Immunofluorescence (IF) staining

For immunofluorescence staining, kidney sections were incubated with solutions containing galectin-3 (Abcam, ab76245, UK) 1:100, Cytokeratin18 (Abcam, ab181597, UK) 1:100, Laminin (Boster, BA1761-1, Wuhan, China) 1:100, γ-H2AX (Proteintech, 29380-1-AP, USA) 1:100, CD41 (Proteintech, 18308-1-AP, USA) 1:100, and CD68 (Cell Signaling Technology, 97778, USA) 1:100, F4/80 (Servicebio, G113373, Wuhan, China) 1:5000, CD34 (Servicebio, GB15013, Wuhan, China) 1:2000, MPO (Servicebio, GB11224, Wuhan, China) 1:5000, NPHS1(Servicebio, GB115714, Wuhan, China) 1:4000,CD31 (Servicebio, GB120015, Wuhan, China) 1:3000, respectively. The fluorescent secondary antibody was stained for 1 h in the darkroom and re-stained by DAPI for 10 min (this step was omitted for platelets). Images were acquired with a fluorescence microscope (Olympus).

Western blot

Total protein was extracted from platelets, cultured cells, or the kidneys of mice using an ice-cold RIPA lysis buffer (Servicebio, G2002, Wuhan, China). The 10% SDS-polyacrylamide gel electrophoresis technique (SDS-PAGE) was employed to separate and purify the protein samples, which were subsequently transferred to a PVDF membrane (Millipore, IPVH00010, USA). The membranes were then blocked with 5% BSA for 1 h. Subsequently, membranes were incubated with GAPDH (Cell Signaling Technology, 5174, USA) 1:1000, PLCγ2 (Cell Signaling Technology, 3872, USA) 1:1000, p-PLCγ2 (Cell Signaling Technology, 3871, USA) 1:1000, Syk (Cell Signaling Technology, 2712, USA) 1:1000, p-Syk (Cell Signaling Technology, 2710, USA) 1:1000, JAQ1 (emfret, M011-0, Germany) 1:1000, BAX (HUABIO, SZ3-07, Shanghai, China) 1:1500, BCL2 (HUABIO, JF104-8, Shanghai, China) 1:2000, NGAL (Proteintech, 26991-1-AP, USA) 1:1000, γ-H2AX (Proteintech, 29380-1-AP, USA) 1:1000 primary antibodies were incubated overnight at 4 °C. HRP-bound secondary antibody bands were detected using ECL (Biosharp, BL520A, Hefei, China). Quantification was conducted using ImageJ software.

RNA extraction and real-time PCR examination

Total RNA was extracted from mouse kidney tissue using Trizol reagent (Vazyme, Nanjing, China). The real-time

PCR assays were performed on a Step One Plus™ system. Primer sequences are shown in Supplemental Table S1.

Cell culture

The mice macrophage cell line Raw264.7 (Pricella, CL-0190, Wuhan, China) was purchased from Wuhan Pricella Life Sciences Co. The mice renal tubular epithelial cell line TCMK-1 (Servicebio, STCC20015P-1, Wuhan, China) was purchased from Sevicebio. The bEnd.3 (QuiCell, B145, Shanghai, China) cell line, immortalized mouse brain endothelial cells, was purchased from Shanghai KuiSai Biotechnology Co. All cell culture procedures were carried out following the manufacturer's guidelines.

Supernatants containing different amounts of damaged TECs were prepared by repeated freezing and thawing of TCMK-1 with liquid nitrogen with or without the addition of 10 μM lactose (MCE, HY-B2123, USA) and platelets were induced by the release of damaged cells.

Platelets co-cultured with Raw264.7

Raw264.7 cells (1×10^6) were seeded into 6-well plates, followed by the addition of washed $Gp6^{+/+}$ or $Gp6^{-/-}$ platelets (1×10^8) for co-culture experiments. Cells were stimulated with galectin-3 (20 μg/L) for 24 h with or without its presence. After removal of platelets by multiple washes with PBS, macrophages were harvested, and their phenotype was analyzed by flow cytometry. For functional evaluation, dextran phagocytosis and cell scratch assays were conducted. In addition, a conditioned medium was applied to trigger apoptosis in renal tubular epithelial cells.

Flow cytometric analysis

Blood specimens were harvested from the orbital venous plexus of mice utilizing heparin-coated capillary tubes and resuspended in PBS. Samples were prepared and tagged with appropriate antibodies, including FITC-anti-mouse-CD62P (BD Biosciences, 555523, USA) for evaluating platelet activation and FITC-JAQ1 (emfret, M011-1, Germany) for assessing GPVI expression on the platelet surface. Peripheral blood from mice was collected, followed by the removal of erythrocytes, and surface staining was carried out with PE-anti-mouse-CD41 (Biolegend, 133906, USA), PE/Cyanine7-anti-mouse-Ly-6C (Biolegend, 128017, USA), PE/Cyanine7-anti-mouse-CD86 (Biolegend, 105014, USA) and PE-anti-mouse-CD206 (Biolegend, 141706, USA) following standardized techniques to analyze platelet-monocyte aggregation and macrophage phenotype. To assess the quantity of apoptotic cells, cells were gathered after a 24 h treatment with conditioned media from various sources. The cell concentration was calibrated to 1×10^6/ml as per the manufacturer's guidelines. A combination of 5 μL FITC and 10 μL PI was introduced to 100 μL of cell suspension, ensuring the staining process was shielded from light for 15 min. Then, 400 μL of Annexin V binding solution was added. The cells were then evaluated using a flow cytometer (BD FACSAria™ III Cell Sorter, Germany), with the resulting data quantified utilizing FlowJo 10.8.1 software.

Phagocytosis assay

Raw264.7 cells were assayed for phagocytosis after co-culture according to the method described above. A master solution of FITC-Dextran (Yeasen, 61220ES10, Wuhan, China) was prepared by dissolving it in sterile PBS to achieve a concentration of 25 mg/mL. Subsequently, 40 μL of this stock solution was pipetted and combined with 960 μL of DMEM culture medium supplemented with 10% serum, resulting in the working solution. Each group of cells, including the control group, was administered 1 mL of the working solution and subsequently incubated in an incubator at 37 °C with 5% CO_2 for 1.5 h, protected from light exposure. Following this incubation period, the cells were collected and centrifuged at 3000 rpm for 5 min. The supernatant was then discarded, and the cells were resuspended in 350 μL of sterile PBS, filtered, and analyzed using a flow cytometer.

Transwell migration and wound healing assay

Transwell chambers with 8-μm pores (Corning, 3422, USA) were utilized to conduct cell migration assays with Raw246.7 cells in a 24-well plate. In these chambers, Raw246.7 cells were placed in the upper layer, while the lower layer was filled with platelets from various sources in the presence or absence of galectin-3 for 24 h. Following this incubation, the cells were fixed using methanol for 30 min and subsequently stained with 0.1% crystal violet for another 30 min. The number of migrating cells was then assessed using a fluorescence microscope. For the bEnd.3 cell wound healing assays, conditioned medium containing platelets co-cultured with Raw246.7 cells was employed. Images of the gaps were captured at 0 h and 24 h, respectively. The migration area was measured with Image J software.

Statistical analysis

Statistical analyses were performed using GraphPad Prism version 10.0. Comparisons between groups were made using t-tests or one-way ANOVAs. Pearson correlation and linear regression were carried out to explore the relationships between parameters. Survival curves were generated using the Kaplan-Meier method and differences between the two groups were evaluated using the Log-rank test. Results were expressed as mean ± SD, based on at least three independent experiments. *P* values below 0.05 were considered statistically significant.

Results

Platelet activity is increased in AKI

To evaluate the changes in platelet activity during AKI, a model of AKI was established through a single intraperitoneal injection of folic acid, with the diagram for inducing FA-AKI presented in Fig. 1A. The results showed that the condition worsened 24 h after folic acid injection, and HE staining revealed the demise of renal TECs, the absence of brush border, and the dilation of tubules. The tubular injury score in model mice was significantly higher than in control mice (Fig. 1A, D). Disease progression was correlated with the levels of blood urea nitrogen (BUN), blood creatinine (CRE) and the kidney/body weight ratio (Fig. 1B, C, E). These findings indicated that the construction of the model was successful. Staining for the platelet-specific marker CD41 indicated higher infiltration of platelets in the kidneys of FA-treated mice (Fig. S1). P-selectin (also known as CD62P) is present within platelet granules in the resting state and is translocated to the platelet membrane upon activation. Flow cytometry results showed significantly elevated CD62P expression on the platelet surface of FA-AKI mice compared to the control mice (Fig. 1F, G). Platelet aggregation and granule release were significantly enhanced in AKI mice under thrombin and collagen stimulation (Fig. 1H-K). In addition, clot retraction and platelet spreading were greater in model mice. Collectively, these findings suggest that platelets exhibit an enhanced capacity for activation, underscoring their critical role in AKI.

GPVI increases in AKI platelets

Activated platelets are essential for the development of inflammation and participate in the inflammatory response through various mechanisms. An important receptor on the platelets surface is GPVI, which has been demonstrated to be crucial in the initial stages of pulmonary thrombotic inflammation in the acute lung injury (ALI) induced by lipopolysaccharide (LPS) [21]. Mice deficient in GPVI and mice treated with anti-GPVI antibody showed protection against lung and systemic damage while no increase in pulmonary hemorrhage. It has been found that rhabdomyolysis-induced AKI, heme released from necrotic myocytes interacting with GPVI to activate platelet, facilitated the formation of ectopic traps in renal macrophages [8]. To explore the function of GPVI in AKI more thoroughly, flow cytometry and Western Blotting tested the expression of GPVI on platelet membranes and its total protein, respectively. The results indicated that the expression levels of platelet GPVI were significantly elevated in FA-AKI mice compared to the control mice (Fig. 2A-D). Similarly, the downstream signaling molecules PLCγ2 and Syk phosphorylation were also significantly elevated (Fig. 2E-G). These results indicated that platelet GPVI upregulated and its downstream signaling was activated during AKI, suggesting that GPVI may play a crucial role in the progression of the disease.

GPVI knockout alleviates folic acid-induced AKI

To investigate the pathological contribution of GPVI to FA-AKI, GPVI knockout (*Gp6*$^{-/-}$) mice were used to assess how the absence of GPVI influences AKI. The knockout of platelet GPVI was verified at the protein level (Fig. S2A). GPVI deficiency did not affect thrombin-induced platelet aggregation but was unresponsive to convulxin stimulation (Fig. S2B-C). In addition, no significant differences were observed in platelet count, mean platelet volume, platelet distribution width and bleeding time (Fig. S2D-G). Meanwhile, the physiological functions of the kidney were not affected (Fig. S2H-J). The results of HE, PAS and Sirius red staining indicated that the lack of GPVI lessened the renal damage and collagen accumulation in FA-AKI (Fig. 3A-C). CRE and BUN assays showed that GPVI deficiency improved renal function (Fig. 3D, E). Folic acid-treated mice exhibited elevated protein and mRNA levels of NGAL, a biomarker of renal tubular injury. In contrast, GPVI knockout demonstrated significant improvement and a reduction in renal cell apoptosis (Fig. 3F-K). Similarly, the positive regions identified through terminal deoxynucleotidyl transferase-mediated dioxyindigo deoxyuridine nick end labeling (TUNEL) assay were significantly diminished in GPVI knockout mice. This observation suggests that the deletion of GPVI may confer a protective effect in FA-AKI. (Fig. 3L, M).

TECs derived galectin-3 induces platelet activation through GPVI pathway

A recent study showed that galectin-3 in cancer cells interacts with platelet GPVI, supporting metastasis of breast and colon cancer cells [10]. Given the common feature of renal TECs death during AKI, damaged cells release many risk-related pattern molecules, which further exacerbate inflammation [22]. Therefore, it was hypothesized that galectin-3, released from renal TECs, interacts with platelet GPVI to further promote the progression of FA-AKI. To test this hypothesis, immunohistochemical staining was performed on renal sections. The findings indicated that galectin-3 levels were significantly elevated in the kidneys of FA-AKI mice compared to the control mice (Fig. 4A, B). The results obtained from ELISA, q-PCR and Western blot were consistent (Fig. 4C-F). Immunofluorescence staining of keratin CK18 and laminin, in conjunction with galectin-3, further confirmed that renal TECs highly expressed galectin-3 compared to other cells during FA-AKI (Fig. 4G, Fig. S3). To further prove our hypothesis, we constructed an AKI cell model using mouse renal TECs TCMK-1 by repeated freeze-thawing in vitro. The

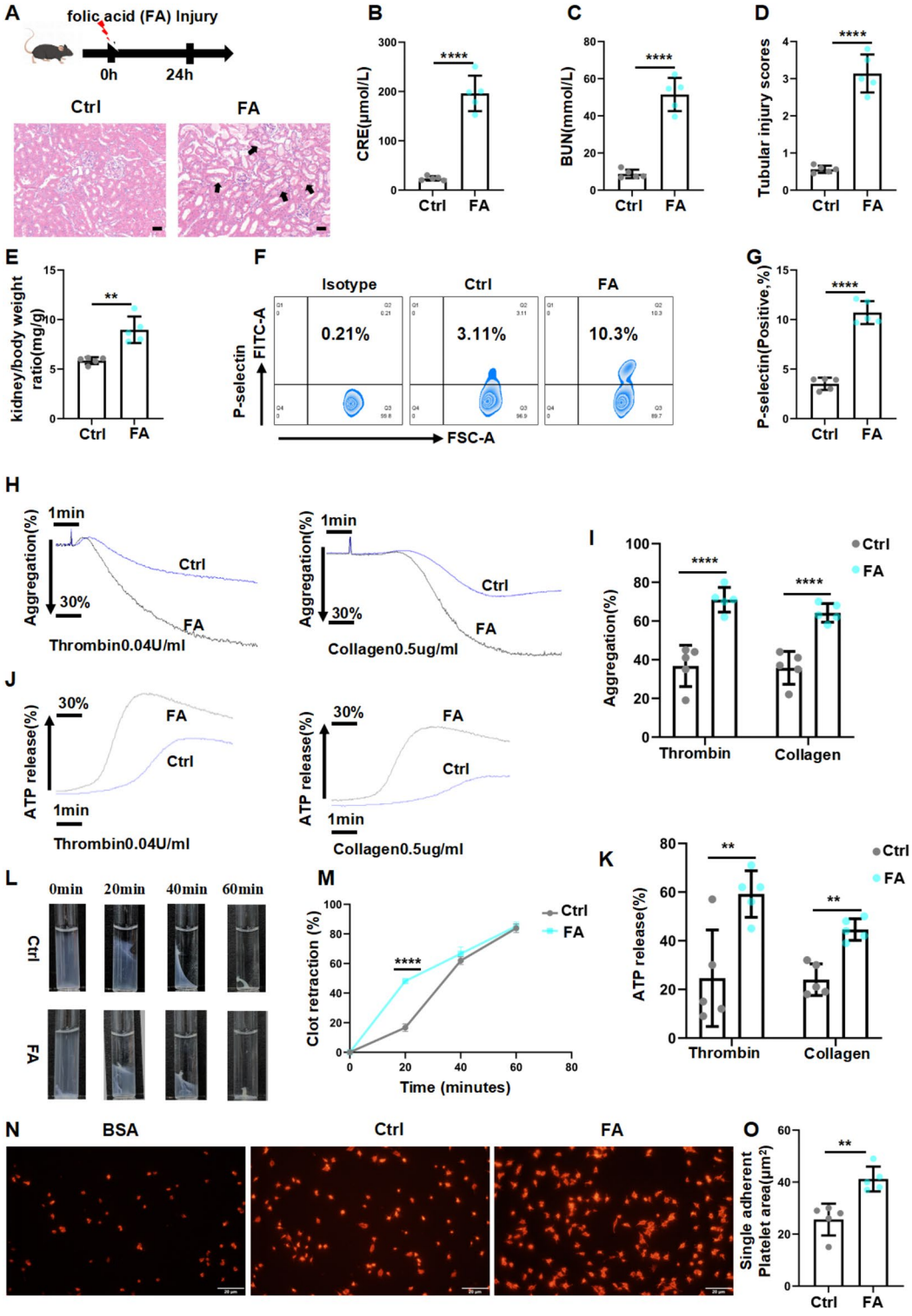

Fig. 1 Platelet activity is increased in AKI. **(A)** The scheme of FA-induced AKI model. Histopathological examination of the kidneys was performed using H&E staining. Arrow indicates renal tubular damage. Scale bars, 50 μM ($n=5$). **(B-C)** Serum creatinine (CRE) and blood urea nitrogen (BUN) levels ($n=5$). **(D-E)** Renal tubular injury scores and kidney/body weight ratio ($n=5$). **(F-G)** Flow cytometry analysis of p-selectin expression in platelets of control mice and FA mice ($n=5$). **(H-I)** Platelet aggregation assay for each group ($n=5$). **(J-K)** Platelet ATP secretion assay for each group ($n=5$). **(L-M)** Representative images of clot retraction at 0, 20, 40, and 60 min ($n=5$). **(N-O)** Representative images of washed platelets spread on fibrinogen. Scale bars, 20 μM ($n=5$). Data are presented as mean ± SD. The statistical tests were performed using t test. $^{*}P<0.05$,$^{**}P<0.01$,$^{***}P<0.001$, $^{****}P<0.0001$ vs. Ctrl. Ctrl, Control; FA, FA-induced AKI

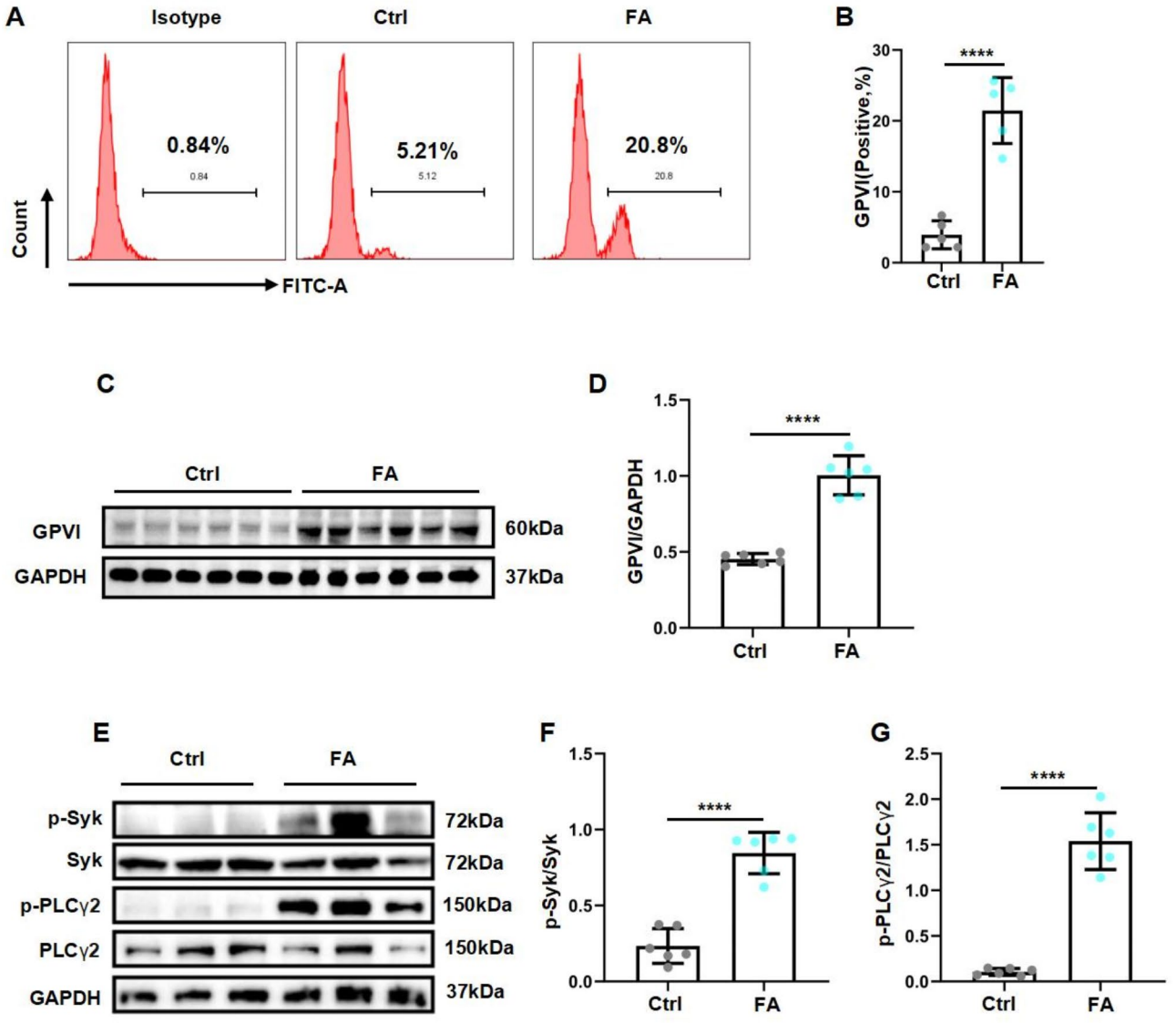

Fig. 2 GPVI increases in AKI platelets. **(A-B)** Flow Cytometry analysis of GPVI expression on platelets of control and FA mice ($n = 5$). **(C-D)** Western blot detection of platelet GPVI protein expression level ($n = 6$). **(E-F)** FA and control platelets were lysed for immunoblotting. Primary antibodies we used included p-Syk, p-PLCγ2, Syk, and PLCγ2 ($n = 6$). Data are presented as mean ± SD. The statistical tests were performed using t test. *$P < 0.05$, **$P < 0.01$, ***$P < 0.001$, ****$P < 0.0001$vs Ctrl. Ctrl, Control; FA, FA-induced AKI

ELISA results showed that damaged renal cell TCMK-1 released large amounts of galectin-3 (Fig. 4H). Previous research has demonstrated that DNA derived from necrotic cells induces platelet activation and enhances the interactions between platelets and granulocytes. This process further exacerbates kidney inflammation and tissue damage [23]. Given the increased platelet activation and elevated GPVI expression in FA-AKI, we aimed to investigate how galectin-3 released from damaged renal cells influences platelet activation. Damaged kidney cell (DTEC) was obtained by multiple freeze-thaw cycles in vitro. Subsequently, mice platelets were incubated with the supernatant derived from DTEC. The analysis of flow cytometry indicated that DTEC supernatant enhanced the expression of P-selectin in a dose-dependent manner. However, this effect was inhibited by lactose, which is known to act as an inhibitor of galectin-3 (Fig. 4I, J). The above results indicated that galectin-3 released from damaged renal TECs contributed to platelet activation. In addition, Western blot analysis revealed that mice platelets induced a CRP-like pattern of tyrosine phosphorylation after galectin-3 stimulation. It was characterized by an increase in phospho-Syk and phospho-PLCγ2. The SFK inhibitor PP2 and the anti-GPVI antibody JAQ1 $F(Ab')_2$ significantly reduced galectin-3-induced phosphorylation of Syk and PLCγ2 signaling (Fig. 4K-M). In conclusion, these results demonstrated that galectin-3 released from injured renal TECs can induce platelet

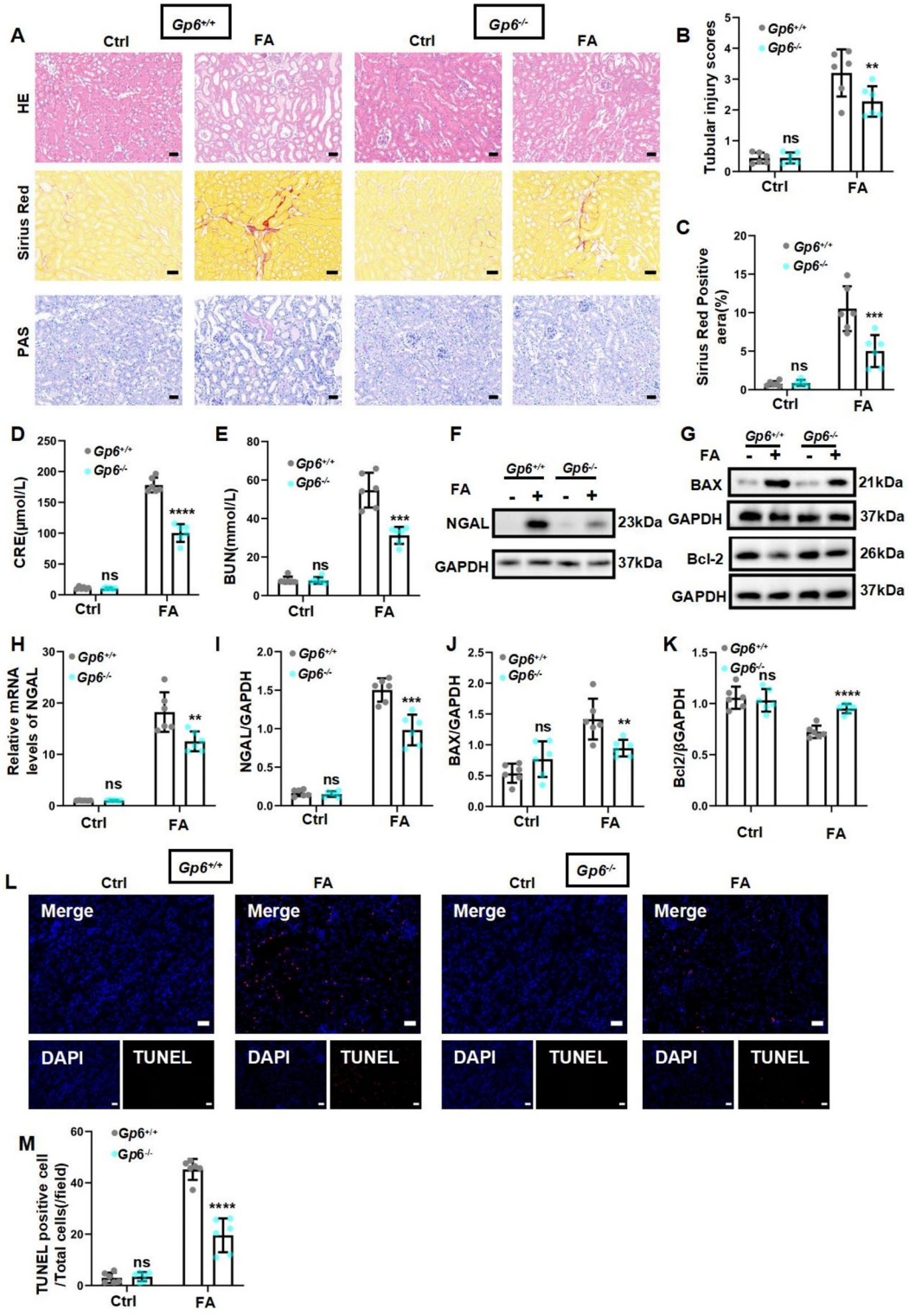

Fig. 3 GPVI knockout alleviates folic acid-induced AKI. **(A-C)** H&E, PAS, and Sirius red staining showed reduced symptoms of epithelial injury in GPVI (*Gp6*) knockout mice after FA-AKI. Scale bars, 50 μM ($n=6$). **(D-E)** Serum creatinine (CRE) and blood urea nitrogen (BUN) levels are decreased in GPVI (*Gp6*) knockout after FA-AKI ($n=6$). **(F, H, I)** Western blot and real-time PCR measured renal NGAL protein and mRNA levels, respectively ($n=6$). **(G, J, K)** Western blots and quantifications of BAX and Bcl2, showing decreased protein levels of BAX and increased levels of Bcl2 in GPVI knockout (*Gp6*) mice after FA-AKI ($n=6$). **(L-M)** TUNEL assay and quantifications showing decreased cell death in GPVI (*Gp6*) knockdown mice after FA-AKI. Scale bars, 50 μM ($n=6$). Data are presented as mean ± SD. The statistical tests were performed using t test. *$P<0.05$, **$P<0.01$, ***$P<0.001$, ****$P<0.0001$ vs. $Gp6^{+/+}$. ns indicates no significance. Ctrl, Control; FA, FA-induced AKI

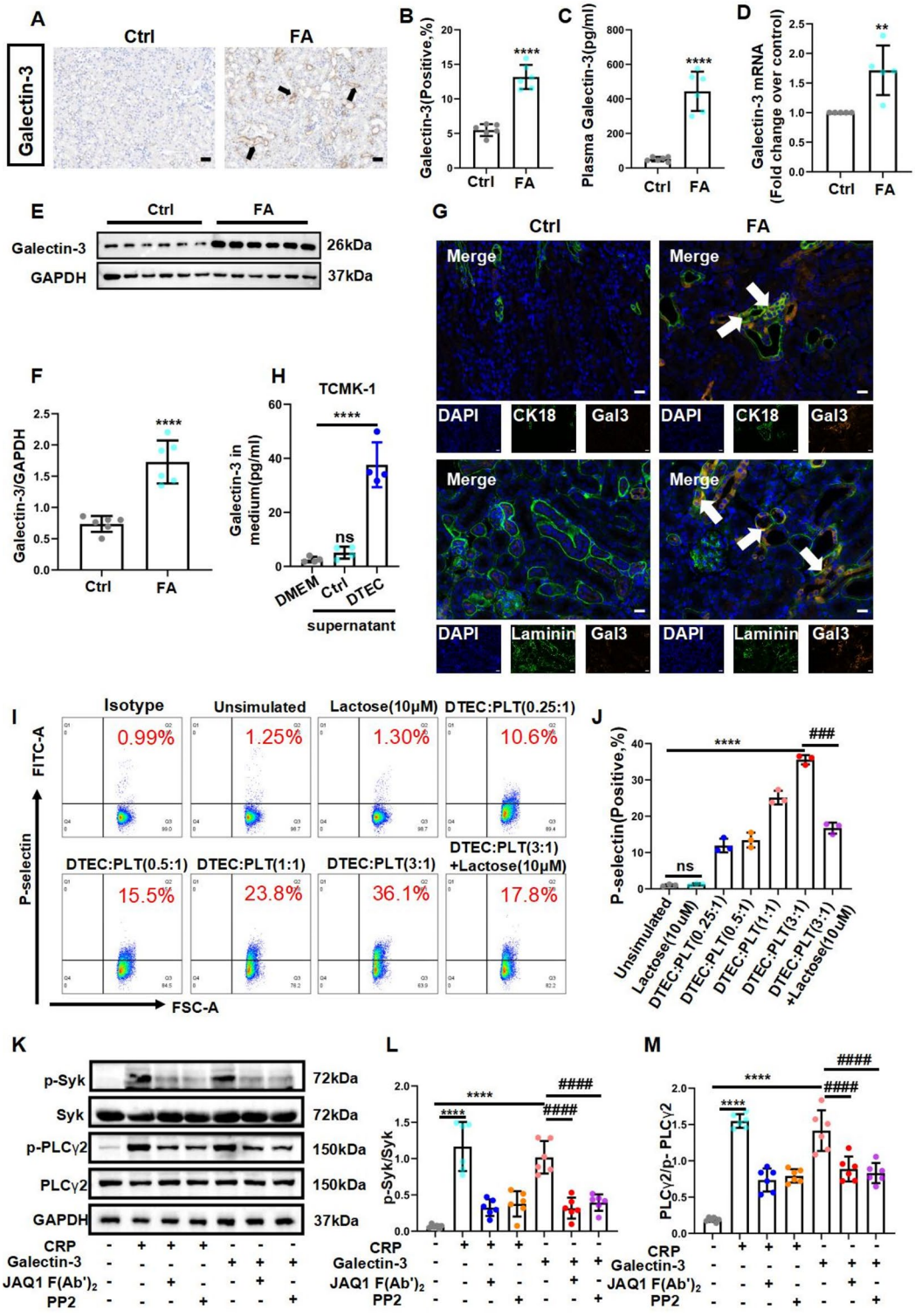

Fig. 4 (See legend on next page.)

activation and trigger its downstream signaling pathways through interaction with platelet GPVI.

The interaction between GPVI and galectin-3 increases MPA in AKI

Consider that activated platelets readily interact with other immune cells in circulation. To validate this, MPA

(See figure on previous page.)

Fig. 4 TECs derived galectin-3 induces platelet activation through GPVI pathway. **(A-B)** Immunohistochemical staining and quantifications of galectin-3 in kidney. Arrow indicates positive staining. Scale bars, 50 μM ($n=6$). **(C-D)** Plasma and mRNA levels of galectin-3 in kidney ($n=5$). **(E-F)** Western blots and quantifications of galectin-3 protein level in kidney ($n=6$). **(G)** Representative images of immunofluorescence staining of keratin CK18 and Laminin with galectin-3 in the kidney after FA-AKI. Arrow indicates co-localization of CK18 and Laminin with galectin3. Scale bars, 20 μM ($n=5$). **(H)** ELISA detection of galectin-3 concentration in TCMK-1 medium under repeated freeze-thawing ($n=4$). **(I-J)** Washed platelets (50×10^6/ml) were stimulated with different volumes of supernatant of damage tubular epithelial cells (DTECs) in the presence or absence of lactate (10μM) and expressed as DTEC: PLT ratio. Platelet CD62p expression was analyzed by flow cytometry ($n=3$). **(K-M)** Western blots and quantifications of protein phosphorylation induced by galectin-3 (20 μg/L) with or without CRP (0.1 μg/ml), JAQ1 $F(Ab')_2$ (20 μg/ml) and PP2 (10μmol/L) pre-treatment ($n=6$). Data are presented as mean ± SD. The statistical tests were performed using t test and one-way ANOVA (J, L and M). *$P<0.05$, **$P<0.01$, ***$P<0.001$, ****$P<0.0001$ vs. Ctrl; ####$P<0.001$ vs. DTEC: PLT (3:1)/galectin-3. ns indicates no significance. Ctrl, Control; PLT, platelet; CRP, collagen-related peptide

characterized by $Ly6C^+CD41^+$ double-positive gates subpopulations were evaluated in flow cytometry, as monocytes are known to be a key driver of FA-AKI. MPA was significantly increased in FA-AKI mice compared with the control mice (Fig. 5A, B), suggesting that activated platelets in FA-AKI readily bind to monocytes. Notably, the $Ly6C^+CD41^+$ cell population was significantly associated with plasma levels of galectin-3 (Fig. 5C). Given the increased expression of platelet GPVI in FA-AKI, the present study aimed to block this receptor to assess its impact on MPA levels. The results showed a significant decrease in MPA levels in AKI after treatment with JAQ1 $F(ab')_2$, a specific inhibitor of platelet GPVI, compared with IgG F(Ab')2 control (Fig. 5D, E). Then, whole blood from GPVI knockout and littermate control mice was collected, and MPA levels were assessed by flow cytometry after stimulation with recombinant galectin-3 protein. The results revealed that MPA levels were significantly elevated in whole blood of galectin-3-stimulated littermate control mice. In contrast, MPA levels were significantly decreased in platelet GPVI knockout mice (Fig. 5F, G). These findings further suggested that galectin-3 interacted with platelet GPVI to promote MPA formation in FA-AKI.

GPVI-galectin-3 interaction polarizes monocytes to M1 pro-inflammatory macrophages

In septic mice, platelets induce monocytes to adopt an M1 phenotype through the GPIb-CD11b pathway in a manner that relies on direct cell-to-cell contact [24]. In contrast, the aggregation of platelets induced by tumor cells enhances the lung metastasis of malignant melanoma through tumor-educated platelets (TEPs). This process leads to the recruitment of tumor-associated macrophages (TAM), contributing to the polarization of TAM towards the M2 phenotype and remodeling the suppressive immune microenvironment within the lung metastases [25]. Monocyte migration is a fundamental process. Therefore, this study aimed to elucidate whether the interaction between galectin-3 and platelet GPVI can induce monocyte migration. As shown in (Fig. 6A, B), in the presence of galectin-3, more Raw264.7 cells cross the polyester membrane in the $Gp6^{+/+}$ group compared to the $Gp6^{-/-}$ group. Pro-inflammatory macrophages (M1-type) are characterized by the secretion of pro-inflammatory cytokines. Its characteristics are the increased levels of CD86 and decreased levels of CD206, which play an essential role in the uptake and destruction of pathogens [26]. In contrast, M2 macrophages have elevated CD206 expression and reduced CD86 levels and play a crucial role in tissue repair by transmitting regulatory signals [27]. Given the functional relevance of macrophage populations in the progression of AKI, platelets were co-cultured with monocytes in the presence or absence of galectin-3 for 24 h. And then platelets were removed by washing. Platelets were observed for their ability to regulate macrophage differentiation, polarization, and function. Before washing, approximately 30% of Raw264.7 coated with platelet aggregation, which was reduced to < 5% after washing (Fig. S2 A, B). It was also investigated whether these effects were influenced by the knockout of platelet GPVI. As shown in (Fig. 6C-E), monocytes co-cultured with 20 μg/L galectin-3, as well as platelets alone, did not induce monocyte polarization. In contrast, the $Gp6^{+/+}$-PLT + galectin-3 group facilitated differentiation towards M1-type macrophages, as evidenced by reduced CD206 levels and increased CD86 expression. Notably, platelet GPVI knockout reversed this effect. On the other hand, the wound healing response of mouse brain microvascular endothelial cells (bEnd.3) to stimulation by macrophage-conditioned medium was evaluated as a readout of the anti-inflammatory M2 response. The experimental flow chart is presented in (Fig. 6F), where the $Gp6^{+/+}$-PLT + galectin-3 group significantly impaired the healing capacity of endothelial cells compared with the control, but platelet GPVI knockout improved the healing capacity (Fig. 6F, G). This implied that GPVI-galectin-3 inhibited the polarization to M2 macrophage. Moreover, FITC-labeled dextran phagocytosis experiments, a classical M1 response, were conducted. Neither platelets nor galectin-3 alone enhanced macrophage phagocytosis. However, the simultaneous presence of $Gp6^{+/+}$-PLT and galectin-3 significantly increased the activity of macrophages. In contrast, the phagocytic activity of macrophages was notably reduced when platelet GPVI was knockout (Fig. 6H, I). These findings suggested that the interaction between galectin-3 and

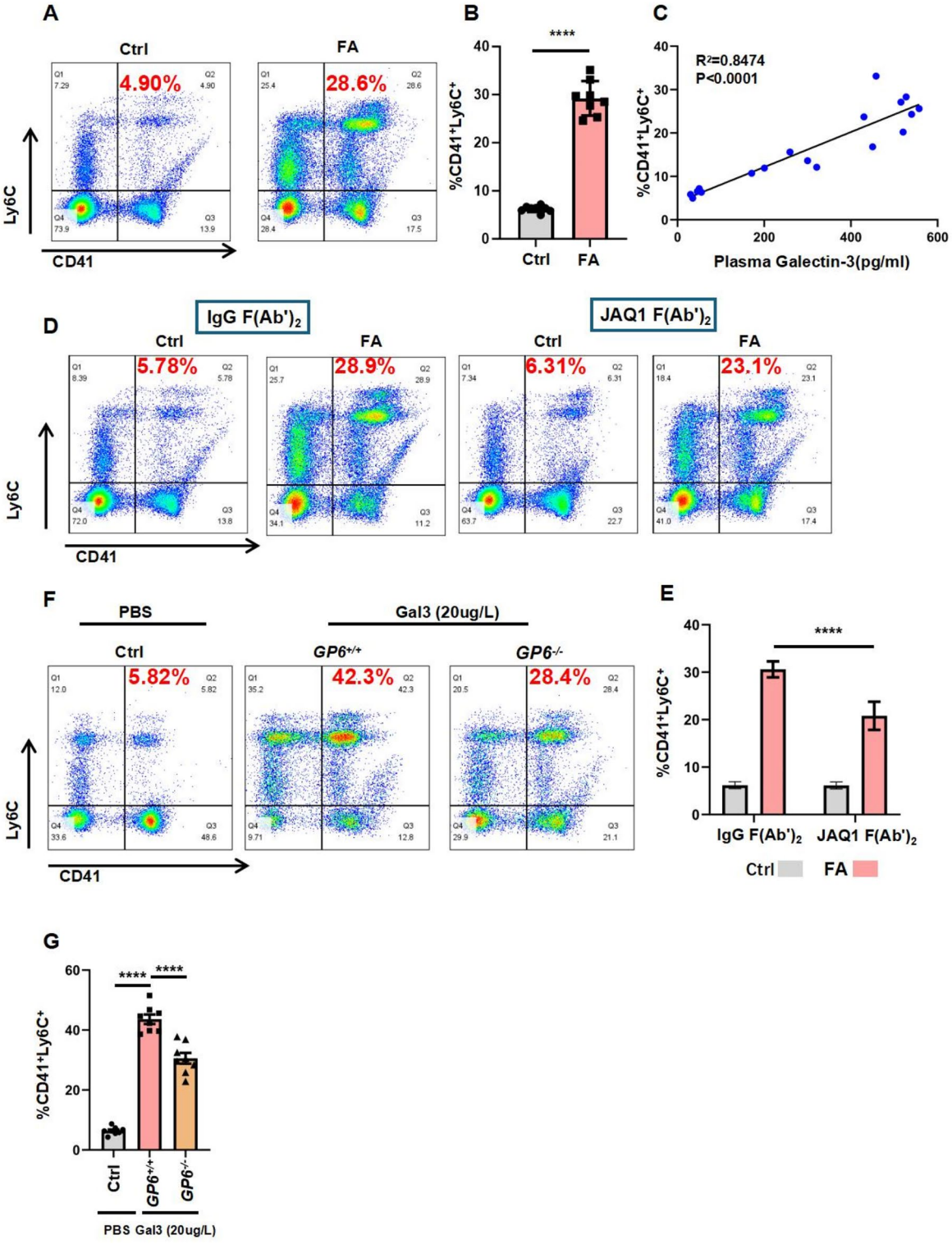

Fig. 5 Interaction between GPVI and galectin-3 increases monocyte-platelet aggregation (MPA) in AKI. **(A-B)** Detection and quantification of MPA ($Ly6C^+CD41^+$) in mice whole blood by flow cytometry ($n=8$). **(C)** Correlation plot between galectin-3 and $Ly6C^+CD41^+$ population. **(D-E)** $Ly6C^+CD41^+$ in Ctrl vs. FA in the presence of control IgG $F(Ab')_2$ or JAQ1 $F(Ab')_2$ (2 μg/g) antibody ($n=5$). **(F-G)** Detection of $Ly6C^+CD41^+$ population in Ctrl, galectin-3 + PLT ($Gp6^{+/+}$) and galectin-3 + PLT ($Gp6^{-/-}$) by flow cytometry ($n=8$). Data are presented as mean ± SD. The statistical tests were performed using t test and Pearson correlation and linear regression (C).$^{****}P<0.0001$ vs. Ctrl/ IgG $F(Ab')_2$/Gal3 + $Gp6^{+/+}$. Ctrl, Control; FA, FA-induced AKI; PLT, platelet; MPA, monocyte-platelet aggregation

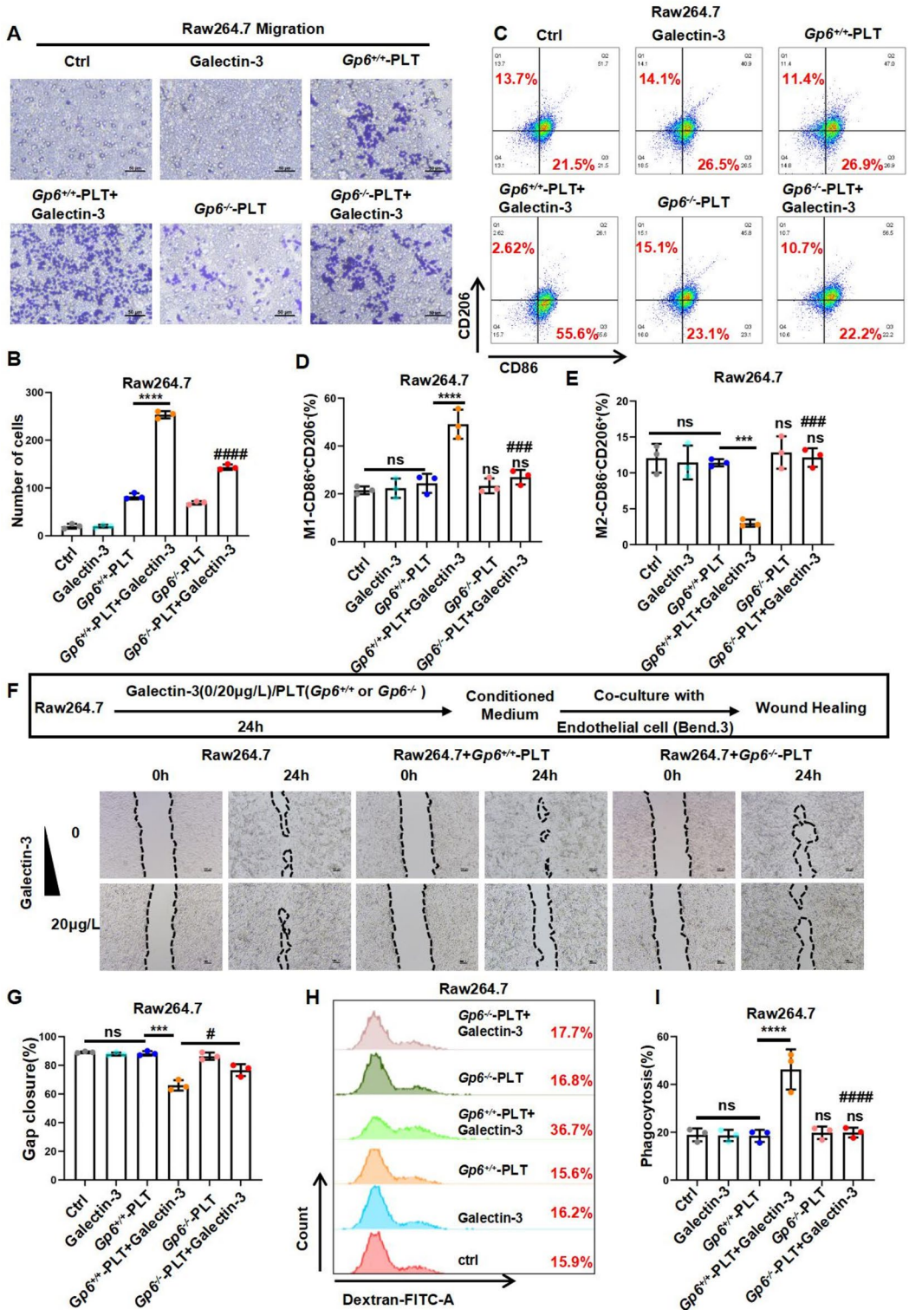

Fig. 6 GPVI-galectin-3 interaction polarizes monocytes to pro-inflammatory macrophages. **(A-B)***Gp6*$^{+/+}$-PLT or *Gp6*$^{-/-}$-PLT induces migration of Raw264.7 with or without of galectin-3 (20 μg/L) ($n = 3$). Scale bars, 50 μM. **(C)** Representative dot plots of CD86 and CD206. **(D-E)** The percentages of **(D)** CD86^{+}CD206^{-}, **(E)** CD86^{-}CD206^{+}, cells are graphed ($n = 3$). **(F)** Conditioned media with *Gp6*$^{+/+}$-PLT or *Gp6*$^{-/-}$-PLT co-cultured with Raw264.7 with or without of galectin-3 (20 μg/L) was used to incubate Bend.3 cell for 24 h to induce wound healing assays. Scale bars, 100 μM. **(G)** Cell migration into the scratched area was calculated by analyzing images with ImageJ software at 0 and 24 h ($n = 3$). **(H-I)** Macrophage phagocytosis of FITC-labeled dextran was assessed, and cell phagocytosis was analyzed by flow cytometry ($n = 3$). Data are presented as mean ± SD. The statistical tests were performed using one-way ANOVA $^{**}P < 0.01$, $^{***}P < 0.001$, $^{****}P < 0.0001$vs Ctrl. $^{\#}P < 0.05$, $^{\#\#}P < 0.01$, $^{\#\#\#}P < 0.001$, $^{\#\#\#\#}P < 0.0001$ vs. *Gp6*$^{+/+}$-PLT + Galectin-3. ns indicates no significance. PLT; platelet

platelet GPVI promoted the polarization of monocytes to an M1 pro-inflammatory phenotype.

MPA induces apoptosis and DNA damage in renal tecs

It was investigated whether the formation of MPA after platelet activation by galectin-3 aggravated AKI. As illustrated in Fig. 7A, Raw264.7 cells were co-cultured with platelets for 24 h in the presence or absence of galectin-3. TCMK-1 was cultured in extracted conditioned medium to assess apoptosis and DNA damage. Flow cytometry and TUNEL staining revealed that supernatants from resting platelets co-cultured with Raw264.7 cells did not induce apoptosis in TCMK-1 cells. However, the apoptosis rate of TCMK-1 significantly increased after the addition of galectin-3 (Fig. 7B-E). In addition, Western blot analysis demonstrated that galectin-3-activated platelets supernatant co-cultured with Raw264.7 cells enhanced the expression of the pro-apoptotic protein Bax in TCMK-1, while decreasing the level of the anti-apoptotic protein Bcl2 (Fig. 7G-H). Histone H2AX is a derivative of histone H2A protein, which is widely used to indicate DNA damage by triggering phosphorylation (γ-H2AX) at the Ser139 site when DNA is damaged. Immunofluorescence and Western blot results showed that supernatants from Raw264.7 co-cultured with platelets with galectin-3 induced DNA damage in TCMK-1 compared with controls (Fig. 7I-L). Together, these results could provide evidence that MPA formation after platelet activation by galectin-3 can drive the progression of AKI.

Blocking galectin-3-GPVI interaction reduces platelet and macrophage infiltration and alleviates AKI

To investigate the interaction between galectin-3 and platelet GPVI in the treatment of AKI, we further explored the role of TD139 in a folic acid-induced GPVI knockout mouse model and the littermate control. TD139 is a galectin-3 inhibitor currently in clinical trials in idiopathic pulmonary fibrosis [28]. As shown in (Fig. 8A), TD139 (15 mg/kg) was administered by intraperitoneal injection 12 h before the folic acid injection. The survival time of mice in the TD139-treated and GPVI knockout groups was significantly prolonged compared with that in the control group (Fig. 8B). In addition, BUN, CRE, tubular injury and collagen deposition exhibited a consistent pattern of improvement. However, the combination of GPVI deficiency with TD139 treatment did not further improve renal function (Fig. 8C-G). Immunofluorescence analysis of mouse kidney tissues showed reduced infiltration of CD41 platelets (yellow) and CD68 macrophages (green) following inhibition of galectin-3 interaction with platelet GPVI (Fig. 8C, H). Furthermore, mRNA levels of inflammatory factors IL-1β, IL-6, and TNF-α were correspondingly decreased in renal tissues (Fig. 8I-K). In conclusion, these findings indicated that blocking the interaction of galectin-3 with platelet GPVI may reduce renal burden and alleviate AKI.

Discussion

Anti-platelet therapy is an adjunctive therapy for AKI and is aimed at mitigating renal dysfunction [29, 30]. It is increasingly recognized that interactions between renal tubular damage, platelets and immune cells are critical drivers of AKI progression, but the complex mechanisms of platelet activation following renal injury remain poorly understood. Our investigation utilizing a folic acid-induced AKI model revealed a significant release of galectin-3 from damaged renal tubules. The galectin-3 interacted with platelet GPVI to activate platelet. This interaction promoted the formation of monocyte-platelet aggregates and induced reprogramming of monocytes to the pro-inflammatory M1 macrophage phenotype, thereby exacerbating AKI. Notably, genetic deficiency of GPVI or application of the galectin-3 inhibitor TD139 ameliorated AKI (Fig. 9). Our study underscores the function of the galectin-3-GPVI interaction in AKI pathophysiology. The results of this study suggested that targeting galectin-3-GPVI interaction may provide a novel therapeutic strategy in AKI treatment.

Platelet GPVI is a crucial platelet surface receptor that plays a vital role in platelet activation and coagulation [5]. Previous studies have shown that under inflammatory conditions, GPVI may also enhance vascular permeability by mediating platelet adhesion to inflamed microvessels [31]. In addition, Saori's study demonstrated that heme-bound platelets GPVI and activated platelets induced macrophage extracellular trap generation to promote rhabdomyolysis-induced deterioration of acute kidney injury [8]. In the present experiments, we found for the first time that platelet hyperactivation in FA-AKI. We further found that platelet membrane receptor GPVI expression was upregulated, and AKI were alleviated in platelet GPVI-specific knockout mice. These results indicated that platelet GPVI played a key role in FA-AKI. However, the mechanism of upregulation of platelet GPVI expression in AKI will be further elucidated in the future.

Renal tubular cells are an important component of the kidney, and their necrosis is one of the main features of AKI [22]. A recent study showed that necrotic renal tubular cells release extracellular DNA to activate platelets, leading to increased platelet and granulocyte crosstalk in disease progression [23]. Galectin-3 is expressed in a variety of cells and regulates intercellular communication. Galectin-3 is a 26 kDa lectin belonging to the galectin family, which is related to β-galactopyranoside [32]. Galectin-3 has a diverse expression and function in renal disease and may exhibit different or even opposite effects in different renal inflammatory conditions. For example,

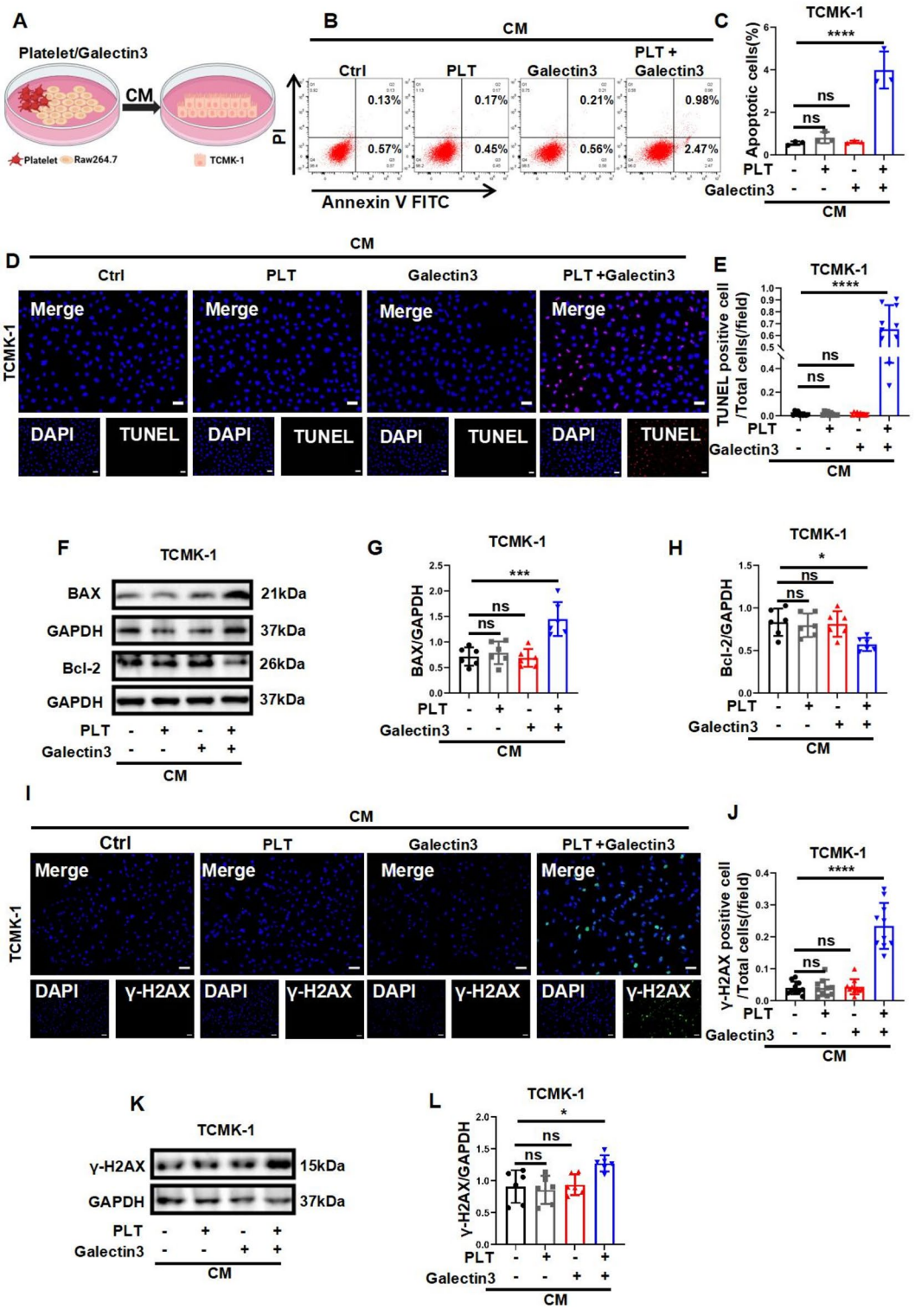

Fig. 7 MPA promotes apoptosis and DNA damage in renal TECs. **(A)** Raw 264.7 cells were co-cultured with platelets with or without of galectin-3 for 24 h and extraction conditioned medium (CM) co-cultured with TCMK-1 for 24 h. **(B-C)** Representative plot of CM-induced apoptosis in TCMK-1 cells detected by flow cytometry (n = 3). **(D-E)** Representative graph of TUNEL assay to detect CM-induced apoptosis in TCMK-1 cells (n=10). Scale bars, 50 μM. **(F-H)** BAX and Bcl2 protein levels were determined by western blot and their quantification in CM-induced TCMK-1 (n = 6). **(I-J)** IF staining of γ-H2AX and quantification (n = 10). Scale bars, 50 μM. **(K-L)** γ-H2AX protein level was determined by western blot and quantitative analysis (n = 6). Data are presented as mean ± SD. The statistical tests were performed one-way ANOVA *P < 0.05, **P < 0.01, ***P < 0.001, ****P < 0.0001 vs P-CM. ns indicates no significance. CM, conditioned medium

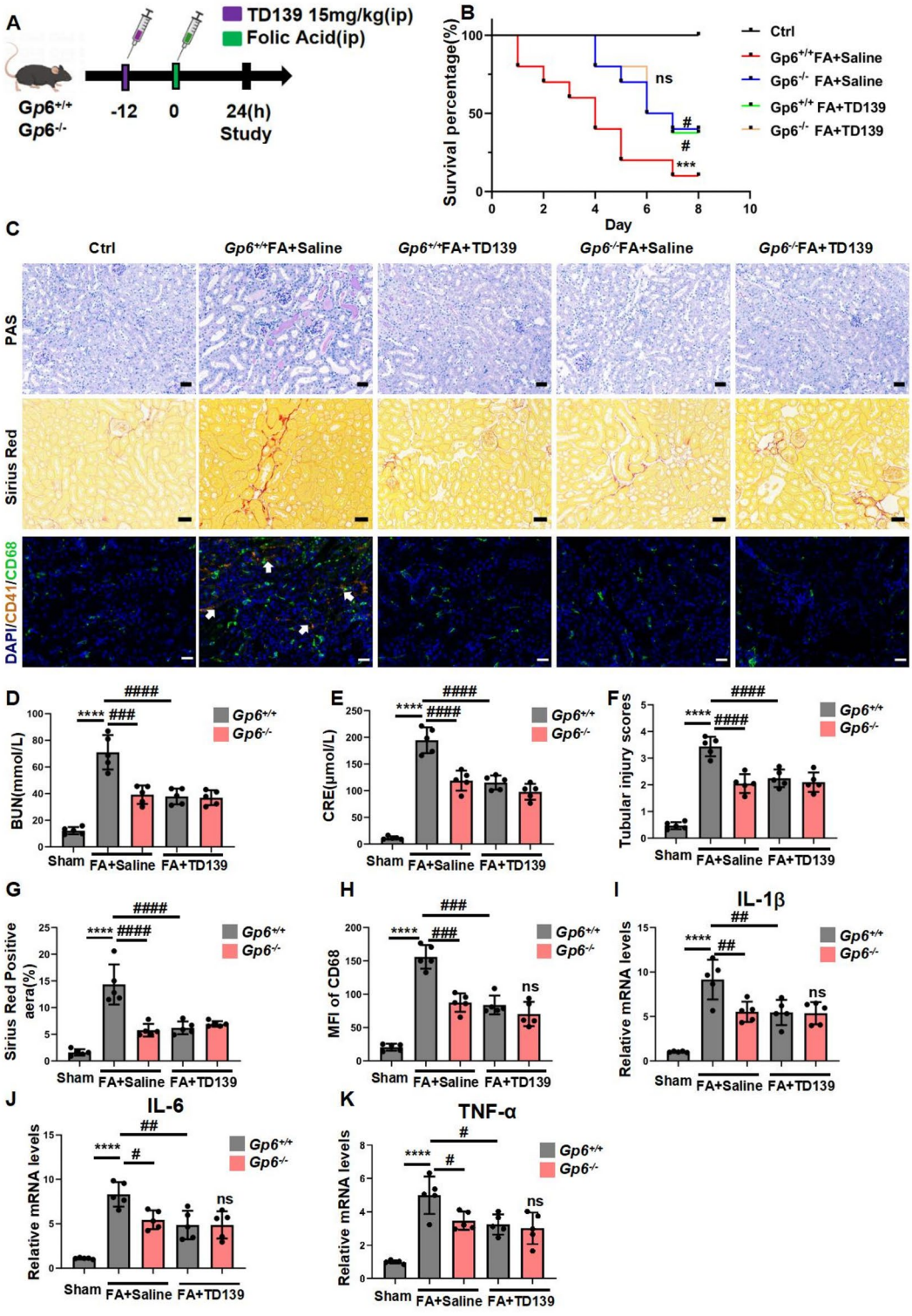

Fig. 8 Blocking galectin-3-GPVI interaction reduces platelet and macrophage infiltration and alleviates AKI. **(A)** Schematic protocol of TD139 treatment in folic acid-induced AKI study using GPVI$^{-/-}$ and GPVI$^{+/+}$ mice. **(B)** 8-day survival was observed, $n = 20$/group. The significance of differences was tested using the log-rank test. **(C)** Representative PAS staining, Sirius Red staining of the kidney. Scale bars, 50 μM ($n = 5$). Representative IF staining of CD41 and CD68 in mice kidney. Arrow indicates positive staining for CD41 platelets (yellow) and CD68 macrophages (green). Scale bars, 100 μM ($n = 5$). **(D-G)** Blood urea nitrogen (BUN), Serum creatinine (CRE) levels and tubular injury scores and Sirius red positive quantification in mice ($n = 5$). **(H)** Mean fluorescence intensity (MFI) statistics of CD68 ($n = 5$). **(I-K)** The levels of IL-1β, IL-6 and TNF-α were determined by qPCR in mice kidney ($n = 5$). Data are presented as mean ± SD. The statistical tests were performed using t test and Log-rank test. ***$P < 0.001$, ****$P < 0.0001$ vs. Ctrl; #$P < 0.05$, ##$P < 0.01$, ###$P < 0.001$, ####$P < 0.0001$ vs. *Gp6*$^{+/+}$FA + Saline. ns indicates no significance. Ctrl, control; FA, FA-induced AKI

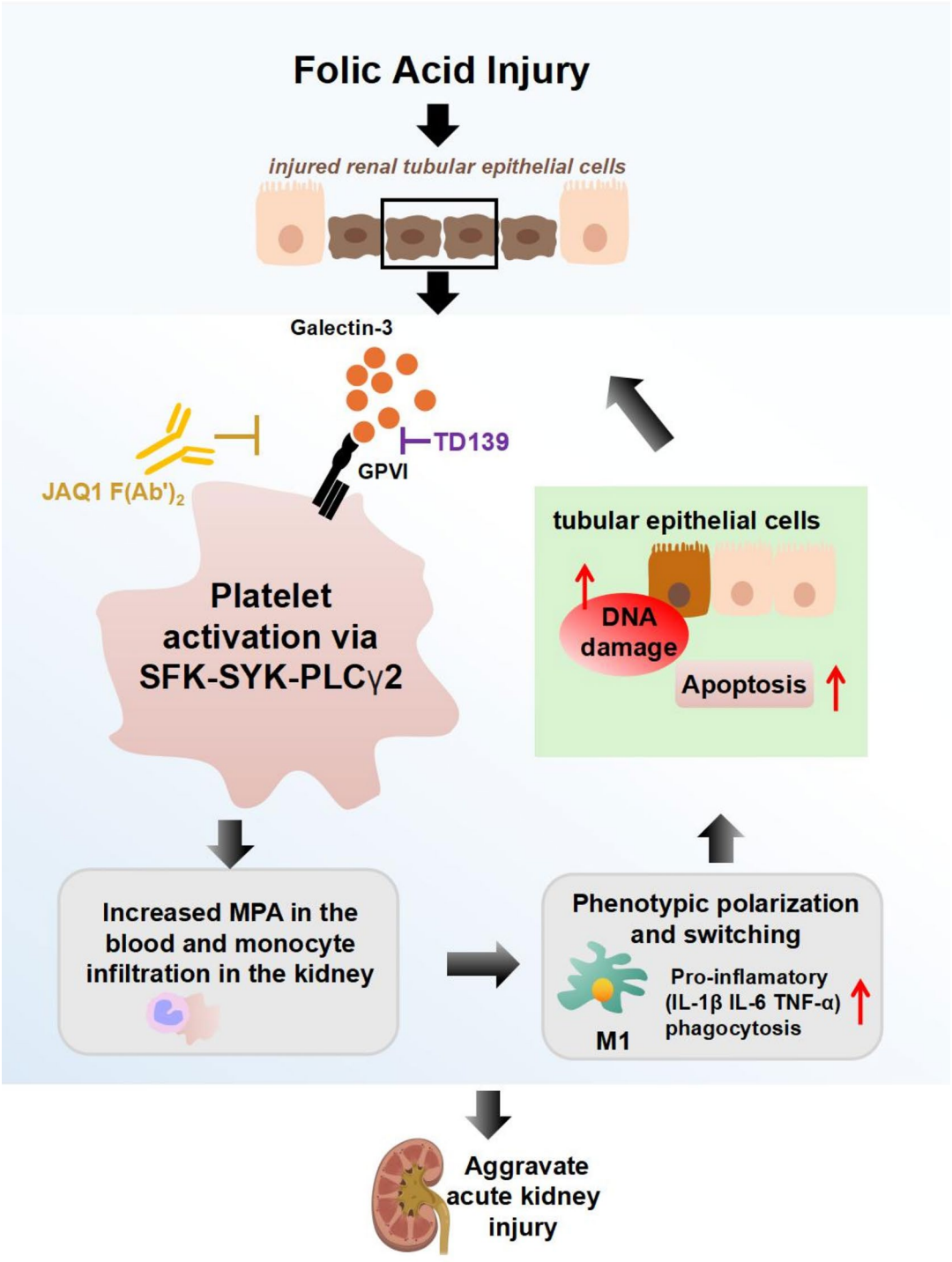

Fig. 9 Overview schedule of Galectin3-GPVI interactions contributing to AKI deterioration

in primary glomerulonephritis, galectin-3 has a potential therapeutic role, whereas in secondary glomerulonephritis caused by systemic lupus erythematosus, galectin-3 may be associated with acute inflammation [33]. Recent studies have shown that tumour cell-derived galectin-3 interacts with platelet GPVI to promote tumour cell metastasis [10]. The expression, localization and role of galectin-3 within the kidney were explored in this study. We found that its expression was significantly elevated in the kidneys of mice suffering from FA-AKI, with immunofluorescence staining verifying its primary localization in renal tubular epithelial cells. In vitro experiments showed that galectin-3, released from damaged renal tubular cells, interacted with platelet GPVI, leading to

platelet activation. In contrast, inhibiting GPVI counteracted the platelet activation triggered by galectin-3. Previous research indicated that the overexpression of galectin-3 notably decreased cell viability and led to cell cycle arrest, and the inhibition of galectin-3 through the use of modified citrus pectin (MCP) mitigated this pro-apoptotic impact and enhanced renal function [34, 35]. Consistent with this, we found that TD139, a potent galectin-3-specific inhibitor, significantly improved renal function in AKI mice. These results may elucidate the renoprotective effects of TD139.

Over the past decade, studies have shown that monocyte-platelet aggregates formed by platelet activation play a key role in inflammation and thrombosis, including cardiovascular disease [36], diabetes [37] and liver cirrhosis [38]. In individuals diagnosed with type 2 diabetes, the levels of MPA are notably elevated compared to healthy individuals. This elevation may serve as an indicator of early inflammation associated with diabetes [37]. Although MPA has the potential to serve as a biomarker for inflammation and thrombosis-related diseases, its presence in circulation, as well as in the kidney following acute kidney injury, has not yet been demonstrated [36]. In our study, it was demonstrated for the first time that the generation of MPA in circulating of mice following folic acid treatment. With Ly6C and CD41 as the markers of MPA formation, it is significantly correlated with plasma galectin-3. The enhancement of apoptosis and DNA damage in renal tubular cells induced by MPA was further corroborated through in vitro experiments. These findings provide the first evidence that MPA exacerbates the progression of FA-AKI.

It has been shown that galectin-3 is involved in the macrophage activation process through interactions with different cell surface receptors such as TLR4 and TREM2 [39]. However, the present study suggested that galectin-3 alone induced limited macrophage polarization. Notably, the interaction of platelet GPVI with galectin-3 significantly enhanced monocyte migration and promoted M1 macrophage polarization. These findings indicated that galectin-3 originating from damaged renal TECs activated platelet, which triggered the MPA formation in FA-AKI. We experimentally demonstrate that MPA formation in the circulation contributes to renal TECs apoptosis and DNA damage in AKI for the first time.

Conclusion

Taken together, galectin-3 derived from damaged renal TECs interacts with GPVI to activate platelets promotes MPA formation and drive macrophage M1 phenotypic switching. This interaction sustains the vicious cycle between platelets, MPA, and TECs injury. Interfering with the interaction of galectin-3 and GPVI to inhibit platelet activation may be a novel therapeutic strategy to ameliorate the progression of AKI.

Abbreviations

AKI	Acute kidney injury
TECs	Renal tubular epithelial cells
FA-AKI	Folic acid-induced acute kidney injury
GPVI	Glycoprotein VI
MPA	Monocyte-platelet aggregation
CRE	Serum creatine
BUN	Blood urea nitrogen

Supplementary Information

The online version contains supplementary material available at https://doi.org/10.1186/s12964-025-02148-5.

Supplementary Material 1

Supplementary Material 2

Supplementary Material 3

Author contributions

Zhang-Yin Ming designed the study, interpreted research data, packaged and revised the manuscript. Ya-Wei Guo carried out experiments, analyzed the data, and drafted the manuscript. Qi Luo and Meng Lu helped with animal breeding and data collection. Rong Ma, Xiang-Bin Zeng and Yu-Min Zhang suggested certain research directions. Yue-Ling Lin and Xu-Ran Guo helped with data curation. All authors approved the final version of the manuscript.

Funding

This work was supported by grants from the National Natural Science Foundation of China (NO. 81970129 and 82370139 to ZY Ming) and Technology Innovation Fund of Innovation Research Institute of Huazhong University of Science and Technology (NO. 2022JYCXJJ040 to YW Guo).

Data availability

No datasets were generated or analysed during the current study.

Declarations

Ethics approval and consent to participate

All animal experiments were approved by the Animal Experimentation Ethics Committee of Tongji Medical College, Huazhong University of Science and Technology.

Consent for publication

Not applicable.

Competing interests

The authors declare no competing interests.

Author details

[1]Department of Pharmacology, School of Basic Medicine, Tongji Medical College and State Key Laboratory for Diagnosis and Treatment of Severe Zoonotic Infectious Diseases, Huazhong University of Science and Technology, Wuhan, China
[2]Hubei Key Laboratory of Drug Target Research and Pharmacodynamic Evaluation, Wuhan, China
[3]Tongji-Rongcheng Center for Biomedicine, Huazhong University of Science and Technology, Wuhan, China

Received: 21 November 2024 / Accepted: 9 March 2025
Published online: 21 March 2025

References

1. Vijayan A. Tackling AKI: prevention, timing of Dialysis and follow-up. Nat Rev Nephrol. 2021;17:87–8.
2. Levey AS, James MT. Acute kidney injury. Ann Intern Med. 2017;167:Itc66–80.
3. Liu BC, Tang TT, Lv LL, Lan HY. Renal tubule injury: a driving force toward chronic kidney disease. Kidney Int. 2018;93:568–79.
4. Jansen MPB, Florquin S, Roelofs J. The role of platelets in acute kidney injury. Nat Rev Nephrol. 2018;14:457–71.
5. Borst O, Gawaz M. Glycoprotein VI - novel target in antiplatelet medication. Pharmacol Ther. 2021;217:107630.
6. Provenzale I, De Simone I, Gibbins JM, Heemskerk JWM, van der Meijden PEJ, Jones CI. Regulation of glycoprotein VI-Dependent platelet activation and thrombus formation by Heparan sulfate proteoglycan Perlecan. Int J Mol Sci. 2023; 24.
7. Mangin PH, Gardiner EE, Ariëns RAS, Jandrot-Perrus M. Glycoprotein VI interplay with fibrin(ogen) in thrombosis. J Thromb Haemost. 2023;21:1703–13.
8. Oishi S, Tsukiji N, Otake S, Oishi N, Sasaki T, Shirai T, Yoshikawa Y, Takano K, Shinmori H, Inukai T, et al. Heme activates platelets and exacerbates rhabdomyolysis-induced acute kidney injury via CLEC-2 and GPVI/FcRγ. Blood Adv. 2021;5:2017–26.
9. Tesfamariam B, Wood SC. Targeting glycoprotein VI to disrupt platelet-mediated tumor cell extravasation. Pharmacol Res. 2022;182:106301.
10. Mammadova-Bach E, Gil-Pulido J, Sarukhanyan E, Burkard P, Shityakov S, Schonhart C, Stegner D, Remer K, Nurden P, Nurden AT, et al. Platelet glycoprotein VI promotes metastasis through interaction with cancer cell-derived galectin-3. Blood. 2020;135:1146–60.
11. Sun H, Jiang H, Eliaz A, Kellum JA, Peng Z, Eliaz I. Galectin-3 in septic acute kidney injury: a translational study. Crit Care. 2021;25:109.
12. Boutin L, Legrand M, Sadoune M, Mebazaa A, Gayat E, Chadjichristos CE, Dépret F. Elevated plasma Galectin-3 is associated with major adverse kidney events and death after ICU admission. Crit Care. 2022;26:13.
13. Scherlinger M, Richez C, Tsokos GC, Boilard E, Blanco P. The role of platelets in immune-mediated inflammatory diseases. Nat Rev Immunol. 2023;23:495–510.
14. Neumann FJ, Zohlnhöfer D, Fakhoury L, Ott I, Gawaz M, Schömig A. Effect of glycoprotein IIb/IIIa receptor Blockade on platelet-leukocyte interaction and surface expression of the leukocyte integrin Mac-1 in acute myocardial infarction. J Am Coll Cardiol. 1999;34:1420–6.
15. Huo Y, Schober A, Forlow SB, Smith DF, Hyman MC, Jung S, Littman DR, Weber C, Ley K. Circulating activated platelets exacerbate atherosclerosis in mice deficient in Apolipoprotein E. Nat Med. 2003;9:61–7.
16. Rudolph TK, Fuchs A, Klinke A, Schlichting A, Friedrichs K, Hellmich M, Mollenhauer M, Schwedhelm E, Baldus S, Rudolph V. Prasugrel as opposed to clopidogrel improves endothelial nitric oxide bioavailability and reduces platelet-leukocyte interaction in patients with unstable angina pectoris: A randomized controlled trial. Int J Cardiol. 2017;248:7–13.
17. Li D, Liu B, Fan Y, Liu M, Han B, Meng Y, Xu X, Song Z, Liu X, Hao Q, et al. Nuciferine protects against folic acid-induced acute kidney injury by inhibiting ferroptosis. Br J Pharmacol. 2021;178:1182–99.
18. Jin X, Chen J, Hu Z, Chan L, Wang Y. Genetic deficiency of adiponectin protects against acute kidney injury. Kidney Int. 2013;83:604–14.
19. Zhi H, Rauova L, Hayes V, Gao C, Boylan B, Newman DK, McKenzie SE, Cooley BC, Poncz M, Newman PJ. Cooperative integrin/itam signaling in platelets enhances thrombus formation in vitro and in vivo. Blood. 2013;121:1858–67.
20. Miao S, Shu D, Zhu Y, Lu M, Zhang Q, Pei Y, He AD, Ma R, Zhang B, Ming ZY. Cancer cell-derived Immunoglobulin G activates platelets by binding to platelet FcγRIIa. Cell Death Dis. 2019;10:87.
21. Burkard P, Schonhart C, Vögtle T, Köhler D, Tang L, Johnson D, Hemmen K, Heinze KG, Zarbock A, Hermanns HM, et al. A key role for platelet GPVI in neutrophil recruitment, migration, and NETosis in the early stages of acute lung injury. Blood. 2023;142:1463–77.
22. Bonventre JV, Yang L. Cellular pathophysiology of ischemic acute kidney injury. J Clin Invest. 2011;121:4210–21.
23. Jansen MP, Emal D, Teske GJ, Dessing MC, Florquin S, Roelofs JJ. Release of extracellular DNA influences renal ischemia reperfusion injury by platelet activation and formation of neutrophil extracellular traps. Kidney Int. 2017;91:352–64.
24. Carestia A, Mena HA, Olexen CM, Ortiz Wilczyñski JM, Negrotto S, Errasti AE, Gómez RM, Jenne CN, Carrera Silva EA, Schattner M. Platelets promote macrophage polarization toward Pro-inflammatory phenotype and increase survival of septic mice. Cell Rep. 2019;28:896–e908895.
25. Chen Y, Zhou J, Liu Z, Wu T, Li S, Zhang Y, Yin X, Yang G, Zhang G. Tumor cell-induced platelet aggregation accelerates hematogenous metastasis of malignant melanoma by triggering macrophage recruitment. J Exp Clin Cancer Res. 2023;42:277.
26. Murray PJ, Allen JE, Biswas SK, Fisher EA, Gilroy DW, Goerdt S, Gordon S, Hamilton JA, Ivashkiv LB, Lawrence T, et al. Macrophage activation and polarization: nomenclature and experimental guidelines. Immunity. 2014;41:14–20.
27. Sierra-Filardi E, Puig-Kröger A, Blanco FJ, Nieto C, Bragado R, Palomero MI, Bernabéu C, Vega MA, Corbí AL. Activin A skews macrophage polarization by promoting a Proinflammatory phenotype and inhibiting the acquisition of anti-inflammatory macrophage markers. Blood. 2011;117:5092–101.
28. Hirani N, MacKinnon AC, Nicol L, Ford P, Schambye H, Pedersen A, Nilsson UJ, Leffler H, Sethi T, Tantawi S et al. Target Inhibition of galectin-3 by inhaled TD139 in patients with idiopathic pulmonary fibrosis. Eur Respir J. 2021; 57.
29. Chappell D, Brettner F, Doerfler N, Jacob M, Rehm M, Bruegger D, Conzen P, Jacob B, Becker BF. Protection of glycocalyx decreases platelet adhesion after ischaemia/reperfusion: an animal study. Eur J Anaesthesiol. 2014;31:474–81.
30. Hu H, Batteux F, Chéreau C, Kavian N, Marut W, Gobeaux C, Borderie D, Dinh-Xuan AT, Weill B, Nicco C. Clopidogrel protects from cell apoptosis and oxidative damage in a mouse model of renal ischaemia-reperfusion injury. J Pathol. 2011;225:265–75.
31. Claushuis TAM, de Vos AF, Nieswandt B, Boon L, Roelofs J, de Boer OJ, van 't Veer C, van der Poll T. Platelet glycoprotein VI aids in local immunity during pneumonia-derived sepsis caused by gram-negative bacteria. Blood. 2018;131:864–76.
32. Bouffette S, Botez I, De Ceuninck F. Targeting galectin-3 in inflammatory and fibrotic diseases. Trends Pharmacol Sci. 2023;44:519–31.
33. Chen SC, Kuo PL. The role of Galectin-3 in the kidneys. Int J Mol Sci. 2016;17:565.
34. Calvier L, Martinez-Martinez E, Miana M, Cachofeiro V, Rousseau E, Sádaba JR, Zannad F, Rossignol P, López-Andrés N. The impact of galectin-3 Inhibition on aldosterone-induced cardiac and renal injuries. JACC Heart Fail. 2015;3:59–67.
35. Fang T, Liu DD, Ning HM, Dan L, Sun JY, Huang XJ, Dong Y, Geng MY, Yun SF, Yan J, Huang RM. Modified citrus pectin inhibited bladder tumor growth through downregulation of galectin-3. Acta Pharmacol Sin. 2018;39:1885–93.
36. Allen N, Barrett TJ, Guo Y, Nardi M, Ramkhelawon B, Rockman CB, Hochman JS, Berger JS. Circulating monocyte-platelet aggregates are a robust marker of platelet activity in cardiovascular disease. Atherosclerosis. 2019;282:11–8.
37. Shlomai G, Haran-Appel T, Sella T, Grossman Y, Hauschner H, Rosenberg N, Grossman E. High-risk type-2 diabetes mellitus patients, without prior ischemic events, have normal blood platelet functionality profiles: a cross-sectional study. Cardiovasc Diabetol. 2015;14:80.
38. Sayed D, Amin NF, Galal GM. Monocyte-platelet aggregates and platelet micro-particles in patients with post-hepatitic liver cirrhosis. Thromb Res. 2010;125:e228–233.
39. Jiang Q, Zhao Q, Chen Y, Ma C, Peng X, Wu X, Liu X, Wang R, Hou S, Kong L, et al. Galectin-3 impairs calcium transients and β-cell function. Nat Commun. 2024;15:3682.

Publisher's note